Food and Bioprocess Technology (2026) 19:248
https://doi.org/10.1007/s11947-026-04322-0

RESEARCH

Enhancing Protein Extraction from *Porphyridium cruentum* using Ultrasound-Assisted Isoelectric Solubilisation and Precipitation

Florencia Cáceres-Ferroni[1,2] · María Salinas-García[1,2] · Silvia Villaró-Cos[1,2] · Elia Rivera-Sánchez[1,2] · Tomás Lafarga[1,2]

Received: 16 January 2026 / Accepted: 12 March 2026 / Published online: 28 March 2026
© The Author(s) 2026

Abstract

This study aimed to optimise a multistep biorefinery process integrating ultrasound-assisted cell wall disruption with sequential pH-driven isoelectric solubilisation/precipitation to maximise compound recovery from *Porphyridium cruentum*. The optimal conditions for the first extraction were pH 8.0 and 100 g·L^{-1}, which achieved the highest release of B-phycoerythrin (4.2 g·100 g^{-1}). Subsequent alkaline solubilisation (pH 12.0) enabled efficient recovery of non-pigment proteins, with precipitation yields maximised at pH 3.8. Reusing the liquid fraction allowed process sustainability to be enhanced without compromising compound recovery. Although an additional acidic extraction step (pH 2.0–2.5) was evaluated, the protein recovery was limited. The resulting fractions displayed distinct functional properties. The B-phycoerythrin-rich fraction imparted colour effectively to model food matrices, obtaining a minimal colour difference of 3.6 for commercial pink gin. The second protein-rich fraction exhibited a high emulsifying capacity and thermal stability at pH 8.0. The third extracted fraction proved to be rich in a wide variety of macro and micronutrients, and the leftovers from these products proved to have potential as plant biostimulants, increasing the seedling vigour index in cucumber (*Cucumis sativus*) seeds by 54–58% compared to water. This integrated approach demonstrates the potential for complete valorisation of *P. cruentum* biomass through a resource-efficient, low-energy process aligned with circular bioeconomy principles.

Keywords *Porphyridium cruentum* · Phycoerythrin · Protein extraction · Sonication · Biorefinery

Introduction

According to recent United Nations projections, the global population will reach nearly 10 billion by 2050 (United Nations, 2024), intensifying pressure on global food systems. At the same time, growing concerns over climate change have accelerated the search for alternative protein sources (Ardila-Leal et al., 2021; Boada et al., 2016), which, combined with increasing ethical awareness regarding animal welfare (Radnitz et al., 2015), have fuelled a rising demand for natural compounds. Microalgae, which transform CO_2 into biomass through photosynthesis, have emerged as a promising alternative to conventional biomass sources because of their rapid growth and their ability to synthesise a wide range of valuable metabolites (Xie et al., 2022).

The red marine microalgae *Porphyridium cruentum* is one of the species that stands out due to the high content of bioactive compounds it can synthesise. These include bioactive phycobiliproteins, exopolysaccharides, chlorophylls, and other carbohydrates (Bernaerts et al., 2018). Phycobiliproteins, comprising phycocyanin (R-PC), allophycocyanin (APC), and phycoerythrin (B-PE), are of great commercial interest. The latter, B-PE, is especially abundant in *P. cruentum*. It is a water-soluble, pink/red fluorescent pigment that has distinctive absorption between 540 and 565 nm and recognised antioxidant, anti-inflammatory, and functional properties (Tsvetanova & Yankov, 2022). Its market importance continues to grow by a projected annual rate of 8.1%, and the forecast is that its value will exceed USD 10.3 million by 2034 (Future Market Insights, 2024). *Porphyridium cruentum* was selected for this study because of its well-documented biochemical composition; this includes a high content of soluble proteins and bioactive compounds, particularly B-PE, which constitutes 5–10% of its dry biomass,

✉ Tomás Lafarga
tomas.lafarga@ual.es

[1] Department of Chemical Engineering, University of Almería, Almería 04120, Spain

[2] Desalination and Photosynthesis Functional Unit, CIESOL Solar Energy Research Centre, Almería 04120, Spain

surpassing the concentrations found in other phycoerythrin-producing species such as the cyanobacteria *Anabaena* sp. and the red macroalgae *Gracilaria gracilis*, which contain about 1.2% and 0.1% of B-PE, respectively (Ghedifa et al., 2021; Nath et al., 2021). In addition, the presence of other valuable compounds enables multiple fractions to be recovered. *P. cruentum* also exhibits a robust growth rate under saline conditions, allowing its production in seawater-based systems, and thus reduces competition for freshwater resources relative to commercially available freshwater microalgae such as *Chlorella vulgaris* and *Arthrospira platensis* (Ferreira et al., 2021; Villaró et al., 2025).

The valorisation of microalgae-derived proteins is still limited, with only a few applications existing in feed and food due to the technical and economic challenges related to their recovery. As a result, many functional proteins remain underexploited, especially in species such as *P. cruentum,* where the target (and most valuable) compound is a pigment. The major limitation to recovering proteins from microalgae lies in the restricted accessibility of intracellular components, largely due to their robust cell walls. Common laboratory-scale lysis strategies include physical techniques like ultrasonication, thermal or osmotic shock, mechanical methods such as high-pressure homogenization or bead milling, and enzymatic and chemical treatments (George & John, 2023). One of the most widely used techniques is sonication, which has to be optimised for each extraction process to reduce energy consumption while obtaining the highest number of disrupted cells (Piera et al., 2024). Beyond disruption, the biochemical composition and the morphological and structural features of the microalga also play a decisive role in protein solubilisation efficiency. Certain proteins are particularly challenging to solubilise due to their hydrophobicity or the presence of disulfide bonds, which reduce solubility. Protein solubility can be significantly enhanced under alkaline conditions, particularly when coupled with controlled denaturation treatments. Once solubilised, protein recovery can be achieved through various precipitation methods, including salting out, organic solvents, or isoelectric precipitation (Grossmann et al., 2018). Of these, the latter was found to be particularly effective as well as being a low-cost method. Isoelectric precipitation is based on adjusting the pH of the solution to a point where most of the proteins carry no net charge, minimising electrostatic repulsion and thereby promoting aggregation and precipitation while preserving functionality (Chen et al., 2019).

Although the recovery of proteins from microalgae has been attempted, the design of a biorefinery scheme that fully valorises the biomass into pigments, proteins, and other fractions of industrial interest is novel. This study sought to optimise the cell disruption concentration to enhance protein release from *P. cruentum* while reducing power use, followed by a fine-tuning of the isoelectric solubilisation/precipitation pH to maximise overall protein recovery. The feasibility of reusing the supernatants from each step was also examined with the aim of enhancing process efficiency and reducing water usage. Finally, the recovered fractions were evaluated for a range of potential applications. A B-PE-rich fraction was assessed for use as a colouring ingredient in selected food matrices; a second fraction rich in other proteins was tested for its potential emulsifying properties across different pH conditions, and the extraction leftovers were examined for their potential as plant biostimulants by measuring their effect on the seedling vigour index. To the best of the authors' knowledge, this is the first protocol that fully valorises *Porphyridium cruentum* biomass into different industrial uses.

Materials and Methods

Microalgal Biomass Used

The *P. cruentum* biomass was produced at the CIESOL Microalgae Demonstration Plant (Almeria, Spain) using tubular photobioreactors. The biomass was harvested by microfiltration, washed with tap water to remove excess salts, frozen, and freeze-dried. The composition of the microalgae in percentages (w/w) was proteins, 31.7%; carbohydrates, 19.6%, lipids, 17.5%, and ash, 31.2%.

Biomass Biorefining

This study aimed to recover two protein-rich fractions — one rich in B-PE and another rich in other proteins. The first step to recover B-PE was to identify the optimal solubilisation pH for this protein. The freeze-dried biomass was resuspended at 100 $g{\cdot}L^{-1}$ in distilled water and the pH was adjusted to 7.0–11.0 using 1 M HCl or NaOH (0.1 for fine adjustment). To disrupt the cell wall, the suspension was then sonicated using a UP400S ultrasonic processor (Hielscher Ultrasonics GmbH, Teltow, Germany) operated at 400 W and 24 kHz. The suspension temperature was kept below 30 °C by cold-water (4 °C) recirculation. Small aliquots of the sample (1 mL) were centrifuged at different sampling points, and the concentrations of R-PC, APC, and B-PE were quantified spectrophotometrically at 565, 620, and 650 nm, as described elsewhere (Tounsi et al., 2024).

After identifying the optimal B-PE solubilisation pH, different biomass concentrations of 1.0 $g{\cdot}L^{-1}$, 10 $g{\cdot}L^{--1}$, and 100 $g{\cdot}L^{-1}$ were evaluated. Aliquots were taken at different time points and the phycobiliprotein concentrations were measured. Ultrasonic-assisted cell disruption was carried out until the concentrations reached a constant value. Higher concentrations were not investigated, as excessively high biomass loadings can substantially increase the viscosity of

the suspension, thereby arresting cavitation bubble dynamics and constraining further improvements in disruption efficiency (Liu et al., 2022).

Ultrasound-Assisted Extraction of B-PE (F-I)

Once the optimal pH and biomass concentration conditions were identified, the disrupted suspension was stirred at 350 rpm for 24 h at 4 °C to ensure the solubilisation of B-PE. This suspension was then centrifuged at 5000 rpm for 10 min using a Digicen 22 centrifuge (Ortoalresa, Madrid, Spain), obtaining a first set of supernatants and non-soluble fractions — Fig. 1.

From the supernatant, a protein fraction rich in B-PE (labelled as F-I) was recovered by precipitation by adjusting the pH to 4.0–4.5. This range corresponds to the isoelectric point of B-PE, where protein aggregation and precipitation are promoted (Koller & Wehrmeyer, 1975), while more acidic conditions could lead to degradation (Munier et al., 2014). The process was completed by stirring for 24 h at 4 °C and was followed by centrifugation. The supernatant was labelled as L-I.

Ultrasound-Assisted Extraction of Protein (F-II)

From the non-soluble fraction, a second solubilisation step was carried out at higher pH values using distilled water, with the pH adjusted to 9.0, 10.0, 11.0, or 12.0. After adjusting the pH, the suspensions were stirred at 350 rpm for 24 h at 4 °C. These suspensions were then centrifuged at 5000 rpm for 10 min using a Digicen 22 centrifuge (Ortoalresa, Madrid, Spain), obtaining a second set of supernatants and a non-soluble fraction labelled as F-III (Fig. 1). The supernatants were rich in proteins that were recovered by isoelectric precipitation by adjusting the pH to 3.0–4.5 using 1 M HCl (0.1 M for fine adjustment). This pH range targets the diverse isoelectric points of the microalgal protein species (Chen et al., 2019). After adjusting the pH, the suspensions were stirred for 24 h at 4 °C to ensure complete solubilisation. The proteins were recovered by centrifugation. This protein-rich fraction was labelled as F-II, and the supernatant was labelled as L-II. More extreme alkaline conditions were not pursued because excessively high pH values are known to compromise protein quality. Under very high alkaline conditions, proteins undergo extensive unfolding and chemical modifications, including hydrolysis and cross-linking (Patel et al., 2025). Such conditions also promote hydrophobic exposure and the formation of lysin-alanine complexes, impairing functionality (Liu et al., 2013). However, a previous work on brewer's grain proteins has shown that pH levels around 11–12 represent an optimal balance by maximising solubilisation while preserving functional properties (Hadinoto et al., 2024).

Valorisation of Protein Recovery Leftovers

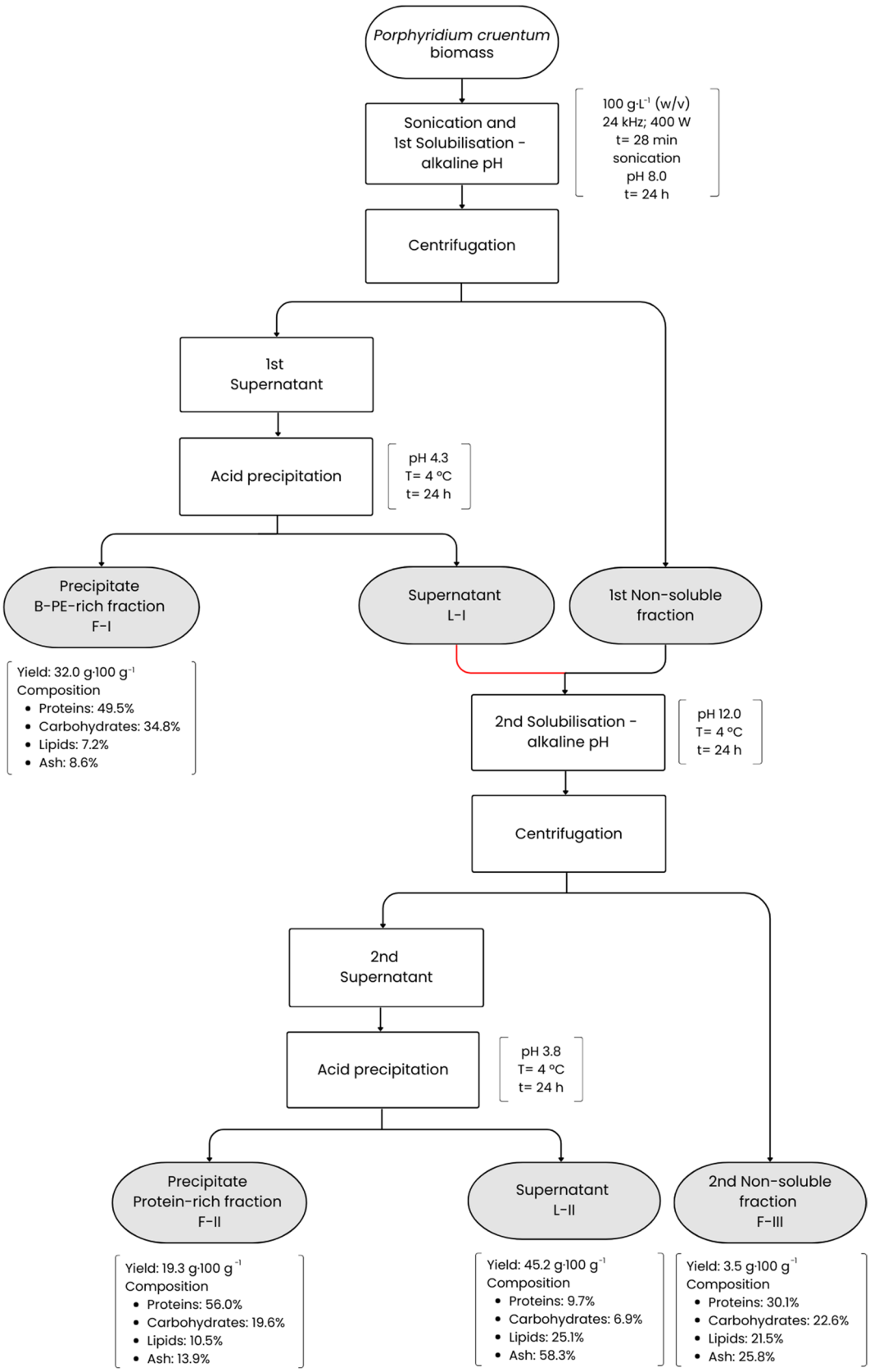
A third solubilisation/precipitation step aimed to fractionate the biomass starting from F-III, as described above (Supplementary Fig. 1). This insoluble fraction was resuspended in distilled water, and the pH was adjusted to 2.0–2.5 with 1 M HCl (0.1 M for fine adjustment) and stirred for 24 h at 25 °C. Some proteins are soluble above the isoelectric point. The extreme acidic shift increases the net positive charge of the protein molecules, generating strong electrostatic repulsion that overcomes protein–protein and protein-polysaccharide interactions within the matrix. This step completes the characterization of the U-shaped solubility profile, ensuring that proteins typically insoluble at neutral or alkaline conditions are solubilised (Damodaran & Paraf, 2017). After centrifugation at 5000 rpm for 10 min, the third supernatant and a non-soluble fraction were collected. The latter, labelled as F-IV, was frozen, freeze-dried, and stored at − 20 °C for further analyses. The pH of the supernatant was then increased to 3.0–4.5 using NaOH 1 M (0.1 M for fine adjustment), and the precipitate, labelled as F-V, was recovered by centrifugation at 5000 rpm for 10 min.

Supernatant Reutilisation

The effect of reusing the liquid fractions (L-I and L-II) during the subsequent solubilisation steps was evaluated as a strategy to recover the solubilised particles present in those fractions and to enhance overall process performance. The recovered liquid fractions were reintroduced into the next solubilisation steps at the same volumes obtained from the previous extraction (Supplementary Fig. 1). Distilled water controls of equal volume were run in parallel. The supernatant reutilisation was assessed in triplicate.

Analytical Determinations

The biomass's total nitrogen content was measured using an ELEMENTAR Vario Micro CHNS elemental analyser (Elementar Analysensysteme GmbH, Hanau, Germany). The total protein content was then estimated applying a nitrogen-to-protein conversion factor of 4.78, as reported in previous studies (Cáceres-Ferroni et al., 2025). The soluble protein concentration in the liquid fractions was determined using Lowry's method (Lowry et al., 1951). The phycobiliprotein content was estimated spectrophotometrically by measuring the optical density at 565, 620, and 650 nm using a UV–Visible Genesys 150 spectrophotometer (Thermo Fisher Scientific, Inc, MA, USA), as described in previous studies (Bermejo-Román et al., 2025). To determine B-PE purity, the ratio of the optical densities measured at 545 nm and 280 nm was used (Bermejo et al., 2001). Purity values lower than 0.7 are considered as food grade, values between 0.7 and


Porphyridium cruentum biomass
Sonication and 1st Solubilisation - alkaline pH
100 g·L⁻¹ (w/v)
24 kHz; 400 W
t= 28 min
sonication
pH 8.0
t= 24 h
Centrifugation
1st Supernatant
Acid precipitation
pH 4.3
T= 4 °C
t= 24 h
Precipitate B-PE-rich fraction F-I
Yield: 32.0 g·100 g⁻¹
Composition
Proteins: 49.5%
Carbohydrates: 34.8%
Lipids: 7.2%
Ash: 8.6%
Supernatant L-I
1st Non-soluble fraction
2nd Solubilisation - alkaline pH
pH 12.0
T= 4 °C
t= 24 h
Centrifugation
2nd Supernatant
Acid precipitation
pH 3.8
T= 4 °C
t= 24 h
Precipitate Protein-rich fraction F-II
Yield: 19.3 g·100 g⁻¹
Composition
Proteins: 56.0%
Carbohydrates: 19.6%
Lipids: 10.5%
Ash: 13.9%
Supernatant L-II
Yield: 45.2 g·100 g⁻¹
Composition
Proteins: 9.7%
Carbohydrates: 6.9%
Lipids: 25.1%
Ash: 58.3%
2nd Non-soluble fraction F-III
Yield: 3.5 g·100 g⁻¹
Composition
Proteins: 30.1%
Carbohydrates: 22.6%
Lipids: 21.5%
Ash: 25.8%

◂**Fig. 1** Process flow diagram of biorefinery scheme. The red line indicates the process optimisation, where the supernatant from the protein precipitation was reused to solubilise the insoluble material. Bracketed values represent the operational conditions applied after optimisation, as well as the corresponding yield and composition of the resulting fractions

3.9 as reagent grade, and values higher than 4.0 as analytical grade (Mittal et al., 2019). The lipid content was determined following the UNE-EN 17908:2024 method based on the Ryckebosch-Foubert procedure (Ryckebosch et al., 2012). Moisture was determined by drying 0.2 g of the sample at 80 °C in an air-flow oven until a constant weight was achieved. To evaluate the ash content, the UNE-EN 17605 standard official method approved by the Spanish Association for Standardisation was used (AENOR, 2022). The total carbohydrate content was calculated by difference. Mineral F-V quantification (Supplementary Fig. 1) was performed using inductively coupled plasma mass spectrometry (ICP-MS) and included Na, Mg, P, S, K, Ca, Cr, Mn, Fe, Cu, and Zn. The samples were previously subjected to microwave-assisted acid digestion to ensure complete mineral release. The resulting digests were analysed using an iCAP TQ ICP-MS system (Thermo Fisher Scientific, MA, USA). All these analytical determinations were carried out in triplicate per natural replicate.

Evaluation of Fraction Properties and Applications

Pigmentation Capacity

F-I was assessed for its potential use as a natural food colourant. Three classes of commercial pink food products were selected: gin, tonic water, and gelatine. For each category, two brands were chosen, and both their pink-coloured and colourless version were obtained for comparative analysis. The selected gins were Beefeater Pink Strawberry (James Burrough Ltd, London, UK) and Larios Rose (Beam Suntory Spain, Segovia, Spain). The selected tonic waters were Schweppes Pink (Suntory Beverage & Food Spain, Madrid, Spain) and Fentimans Rose (Fentimans Ltd, Northumberland, UK). The gelatine products were AllPura Red Fruits (DietMed Spain SLU, Madrid, Spain) and Royal Watermelon (Mondelez España Commercial SL, Madrid, Spain). For the tonic water, a degassed treatment was applied by stirring the sample for 5 min at 350 rpm.

The potential of F-I to mimic the commercial product's colour was determined by adding known amounts of F-I (pH 8.0) at a known concentration into the colourless matrices and measuring the resulting colour modifications. Colour measurements of the samples were performed using the CIELAB system and a CR-400 chroma meter (Konica Minolta, Tokyo, Japan) with the D65 illuminant. The extract was added while the mixture was being continuously stirred. The procedure was repeated until the pink hue was as close as possible to that of the commercial pink food. All colour measurements were performed in triplicate per sample, as described in a previous study (Villaró et al., 2023).

Emulsifying Capacity

The emulsifying capacity of F-II was assessed across different pH values following a method described elsewhere, with slight modifications (Garcia-Vaquero et al., 2017). Briefly, a 1.5% (w/v) protein solution was prepared and adjusted to pH 2.0–10.0, after which sunflower oil was incorporated at a 3:2 (v/v) oil-to-aqueous ratio. The emulsions were generated by homogenisation at 15,000 rpm for 1 min using a T-25 ULTRA-TURRAX® (IKA, Staufen, Germany) and subsequently centrifuged at 5000 rpm for 5 min. The emulsion volumes before and after centrifugation were recorded to determine the emulsifying capacity. To evaluate thermal stability, the emulsions were heated at 85 °C for 15 min, cooled at room temperature for 10 min, and centrifuged again under identical conditions. The emulsifying capacity and stability of F-II were determined in triplicate. Commercial potato protein isolate (Moara, Madrid, Spain) was selected as a comparative control for the emulsifying capacity assay since the well-documented interfacial properties of this protein and its established presence in the food ingredient market make it a high-performance plant-based benchmark (Alting et al., 2011; Schmidt et al., 2018). Although the biological sources and structural configurations of these proteins differ, using an established plant-based isolate provides a rigorous reference point for evaluating the industrial competitiveness of the microalgal fraction.

Evaluation of Plant Biostimulant Activity

The seedling vigour index of F-III and L-II was determined using cucumber (*Cucumis sativus*) and basil (*Ocimum basilicum*) seeds, as described in a previous work, with slight modifications (Chabili et al., 2025; Morillas-España et al., 2024). The cucumber plant is a species traditionally employed in experimental testing for evaluating the potential impacts of substances on seedling emergence and early growth, due to its rapid growth kinetics and sensitivity (OECD, 2006). Basil is a high-value aromatic crop that is economically important because of its essential oil profile. However, industrially, it requires high germination rates and the establishment of a rapid, uniform stand to be produced successfully (Biró-Janka et al., 2019). As warm-climate species characterised by high metabolomic rates, both cucumber and basil serve as ideal 'fast-track' physiological models to evaluate the potential of *P. cruentum* extracts to act as early growth promoters. Briefly,

the samples were suspended in distilled water at a final concentration of 0.5 g·L^{-1}. To evaluate plant biostimulant activity, 0.8 mL of either distilled water (the negative control), microalgae extract, or gibberellic acid solution (the positive control, 1 mg·L^{-1}) was added to a Whatman No. 5 filter paper placed inside sterilised Petri dishes. Then, 25 commercial cucumber and basil seeds were placed on the filter paper. The seeds were then incubated for 3 days at 25 °C in darkness. Seeds were considered germinated when the radicle length exceeded 2 mm (Chabili et al., 2025). Since the seedling vigour index integrates both the rate and uniformity of germination along with the morphological development of the seedling, the incubation time point was selected to ensure accurate morphological measurement before the onset of spatial and resource competition between seedlings (Hampton & Tekrony, 1995). By assessing the initial post-germination stage, one can detect early growth-promoting responses while avoiding confounding effects from density or nutrient limitation. Each treatment was performed in triplicate.

Statistical Analysis

The data are presented as the mean ± standard deviation (SD). Statistical evaluation was performed using a one-way ANOVA followed by Fisher's LSD post hoc test ($p < 0.05$) using Statgraphics Centurion v19 (Statgraphics Technologies Inc., VA, USA) software.

Results and Discussion

Ultrasound-Assisted Recovery of Phycobiliproteins

Figure 2A illustrates the phycobiliprotein concentrations obtained after sonication under different solubilisation pH conditions.

The highest yield was obtained at pH 8.0 (4.5 g·100 g^{-1}), showing a significant difference to the other pH conditions ($p < 0.05$). The observed decline at alkaline pH values correlates well with the reduced absorbance at 565 nm (Fig. 2B). It is also in line with previous reports, where the

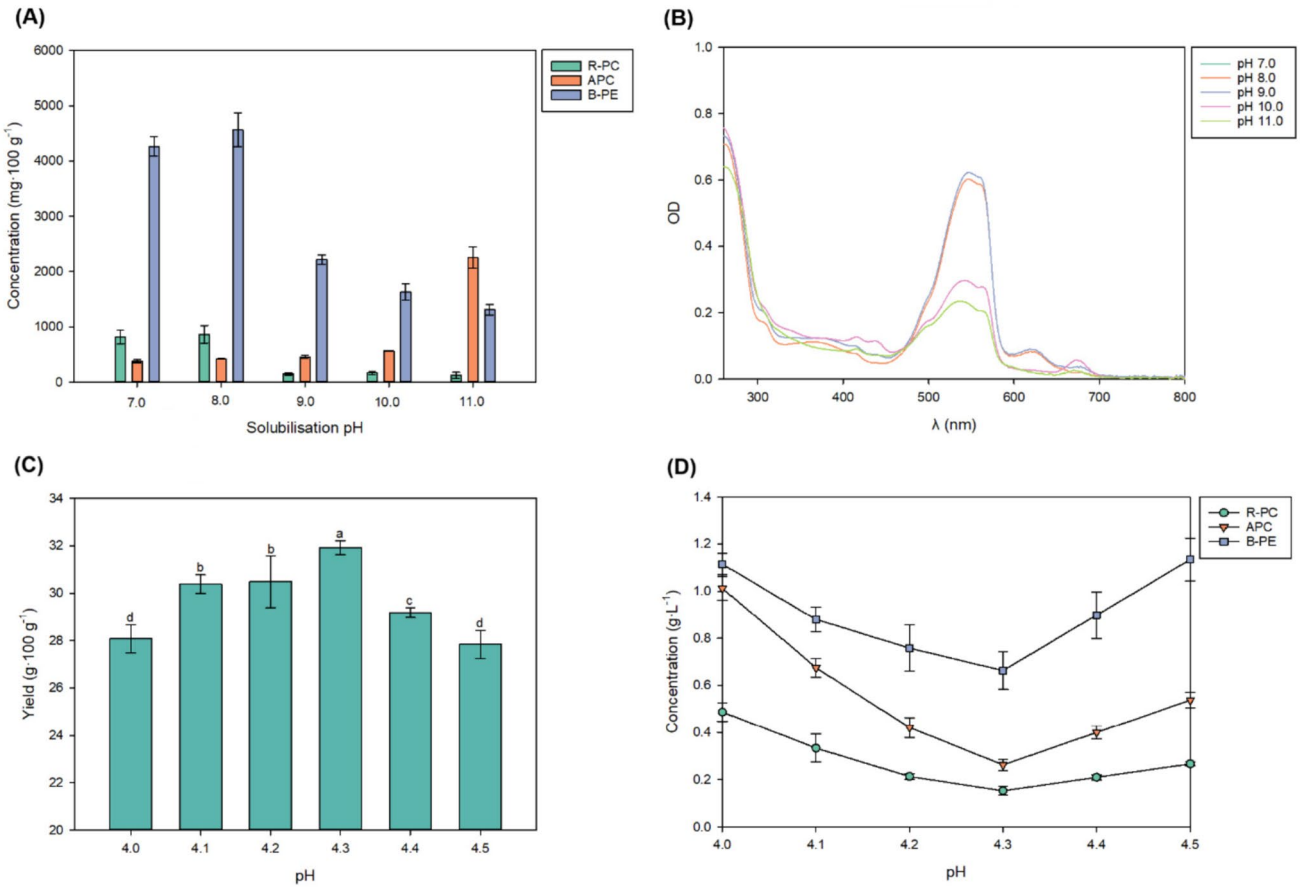


Fig. 2 First extraction. **A** Effect of pH on the solubilisation of phycobiliproteins; **B** UV–Visible spectra (260–800 nm) at different pH values; **C** effect of precipitation pH on the recovery yield; and **D** effect of pH on phycobiliprotein concentrations in the supernatant during the precipitation step. Values correspond to the mean of three independent measurements ± SD

B-PE concentration was stable at pH 7.0–8.0, whereas at pH 11, a decrease in B-PE absorbance intensity was detected (Munier et al., 2014). Extreme pH values can disrupt the electrostatic interactions and hydrogen bonding that stabilise protein assemblies, leading to chromophore structural alterations. Conversely, pH values around 7.0–8.0 preserve the oligomeric state (Munier et al., 2014). After identifying 8.0 as the optimal extraction pH, the effect of biomass concentration on energy demand was assessed. At 100 g·L^{-1}, the maximum B-PE concentration (4.2 g·100 g^{-1}) was achieved with an energy utilisation of 26.8 MJ·kg^{-1} after 28 min of sonication. To achieve the same B-PE recovery using suspensions at 10.0 and 1.0 g·L^{-1}, the energy requirement was 268 and 1,152 MJ·kg^{-1}, respectively. This represented 10- and 42-fold higher energy inputs ($p < 0.05$). These results are consistent with previous reports in which the minimum energy required for comparable cell wall disruption occurred at the highest concentration tested (100 g·L^{-1}) (Chegukrishnamurthi et al., 2025). The reduced power consumption observed at higher biomass concentrations can be attributed to greater ultrasonic cavitation efficiency under these conditions. In concentrated suspensions, a greater number of cells are available per unit volume to interact with the cavitation events, thereby maximising the conversion of applied energy into mechanical disruption and pigment release, while minimising energy dissipation as heat or turbulence in the medium. Elevated biomass loadings enhance cavitation-cell interactions and markedly improve energy efficiency (Liu et al., 2022).

The B-PE contained in the supernatant was recovered by precipitation. The yield obtained from the different treatments showed a significant difference between treatments, indicating a strong dependence on pH ($p < 0.05$). The F-I recovery yield reached a maximum at a precipitation pH of 4.3, corresponding to 32.0 g·100 g^{-1} of biomass. The recovery yield of B-PE was 1.2 g·100 g^{-1} of biomass; the F-I extract had a purity of 1.7, meaning it can be considered as reagent grade. At pH values higher than 4.3, the recovery yield decreased with values dropping to 29.0 and 28.0 g·100 g^{-1} at pH 4.4 and 4.5, respectively (Fig. 2C). These results are consistent with the observed solubilisation of phycobiliproteins in the supernatant (Fig. 2D), where the lowest protein concentration in the supernatant corresponded to the highest recovery yield ($p < 0.05$). In the present work, the isoelectric point (4.3) obtained for B-PE from *P. cruentum* is in close agreement with the results reported for this same protein from the red alga *Rhodella violacea*, in which two isoproteins of B-PE exhibited isoelectric points of 4.4 and 4.2 (Koller & Wehrmeyer, 1975). The acidic isoelectric point observed for B-PE from *P. cruentum* arises from its high acidic residues content, notably aspartate and glutamate. In both the α- and β-subunits, several aspartate residues are positioned near the propionic groups of the covalently bound phycoerythrobilin chromophores, where they form stabilising salt bridges with nearby basic residues such as arginine and lysine. These interactions lower the pKa of the acidic chains (~2), keeping them predominantly deprotonated and negatively charged at neutral pH. Although there are exceptions, the extensive network of deprotonated acidic residues is primarily responsible for the protein's pronounced negative charge and the need for a low pH to neutralise this net charge, resulting in its acidic isoelectric point (Camara-Artigas et al., 2012). Overall, F-I contained a high protein content and a B-PE purity that enables its use as a reagent. Its purity could be further improved through additional purification steps to remove salts and other non-protein components. This will be attempted in future research.

Protein Recovery from Phycobiliprotein-Extraction Leftovers

Figure 3A shows the protein solubilisation under different alkaline pH conditions. The protein concentration increased with pH, ranging from approximately 8.6 g·100 g^{-1} at pH 9.0 to a maximum of 10.0 g·100 g^{-1} at pH 12.0 ($p < 0.05$). Moreover, the phycobiliprotein concentration increased with pH, with a marked rise in APC at pH 12.0. The UV–Visible scans presented in Fig. 3B corroborate these findings, showing higher optical densities as the pH increased, with characteristic peaks at 420 and 680 nm. These results indicate the co-extraction of carotenoids and chlorophyll a, respectively. These lipophilic pigments are co-extracted alongside phycobiliproteins under strong alkaline conditions. Similar trends have been reported in *C. vulgaris*, where pH 12.0 enabled the maximum protein extraction after two homogenization cycles (Kulkarni & Nikolov, 2018). Likewise, Nissen et al. (2021) reported that, for a 10.0 g·L^{-1} of alfalfa protein suspension, protein solubility increased progressively with rising pH, roughly doubling when comparing neutral conditions (pH 7.0) to strongly alkaline conditions (pH 12.0).

The observed effect can be explained by protein denaturation and charge-driven solubilisation. At pH values far from the isoelectric point, proteins acquire net negative or positive charges on their amino acid residues, promoting electrostatic repulsion between molecules. This reduces aggregation and weakens non-covalent interactions such as hydrophobic forces and hydrogen bonding that normally restrict solubility. This, in turn, facilitates protein release from the biomass matrix. Extensive hydrolysis or cross-linking reactions are unlikely at the experiment temperature (Camara-Artigas et al., 2012).

The simultaneous presence of allophycocyanin and lipophilic pigments at pH 12.0 reflects the disruption of the thylakoid and phycobilisome structures. Allophycocyanin release indicates the disassembly of the phycobilisome core, while chlorophyll-a and carotenoids, normally embedded in

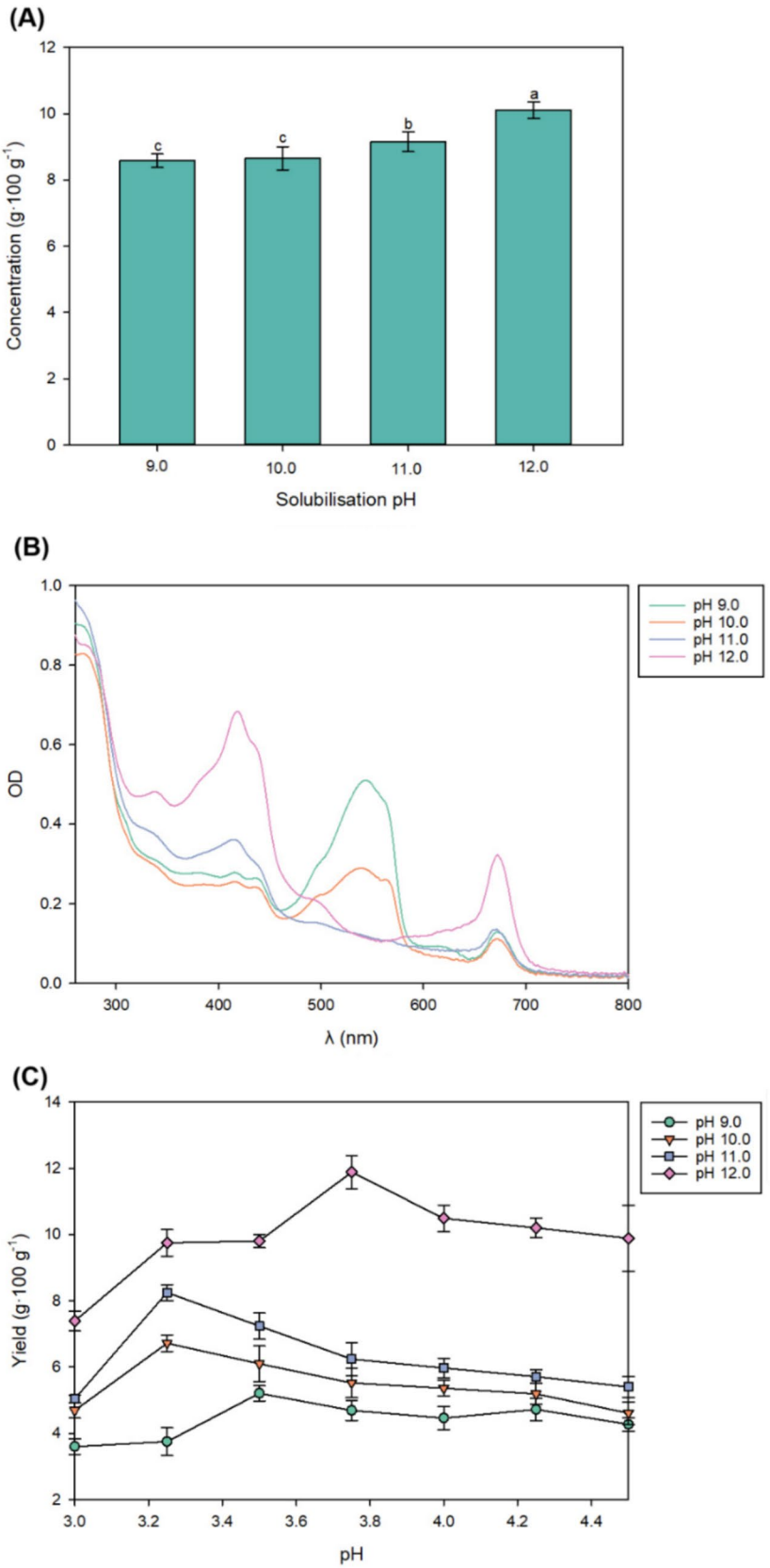


Fig. 3 Second extraction. **A** Effect of alkaline pH on protein solubilisation; **B** UV–Visible spectra of the extracts in the 260–800-nm range at different alkaline pH values; and **C** effect of precipitation pH on yield during the alkaline step. Values correspond to the mean of three independent measurements ± SD

membrane lipids, are co-extracted. This is because a pH of 12.0 acts similarly to detergent action, destabilising pigment-membrane interactions and promoting lipid hydrolysis, thus enabling both hydrophilic and lipophilic pigments to partition into the aqueous phase (Glazer, 1989).

The proteins that solubilised at alkaline pH values were recovered by isoelectric precipitation. The recovery yields of the protein-rich fraction (F-II) at different pH values in the second extraction are shown in Fig. 3C. The yields differed significantly between treatments ($p < 0.05$). The maximal yields were consistently achieved at precipitation pH values between 3.2 and 3.8, with yields declining progressively as the precipitation pH approached 4.4. The highest yield of 12.1 g·100 g^{-1} was achieved at a solubilisation pH of 12.0 with a protein content of 5.5 g·100 g^{-1}, whereas at a solubilisation pH of 11.0, 10.0, and 9.0, the protein content of the fractions was 3.0, 2.4, and 1.8 g·100 g^{-1}, respectively. A similar trend was found in a previous study where the protein extraction was markedly higher at pH 12.0 compared to pH 9.0–11.0 for *P. purpureum*, leading to a rise in the recovery yield from 2.5 to 3.0 g·100 g^{-1} when the pH was increased from 9.0 to 12.0 (Stack et al., 2018).

The non-soluble fraction from the protein recovery was resuspended under acidic conditions for a third protein solubilisation step. As one can see in Fig. 4A, the lower the pH, the higher the optical density.

These results are consistent with those observed for *Arthrospira platensis* proteins, where solubility was 5.9% at pH 2.0, dropping to 0.0% at pH 4.0, near their isoelectric point (Taragjini et al., 2022). Such results can be explained by acid-induced changes in the protein charge and partial hydrolysis. Under strongly acidic conditions, additional protonation occurs, lowering the effective pKa of acidic side chains (to ~ 2.0), which modifies protein charge distribution and enhances solubilisation. Simultaneously, partial protein hydrolysis can be induced, breaking peptide bonds, generating smaller fragments and exposing hydrophobic and charged groups (Dai et al., 2019). The combination of acid-induced protonation and partial hydrolysis facilitates protein dispersion in solution, explaining the increased solubility observed at pH 2.0 for *P. cruentum* proteins.

The proteins solubilised under acidic conditions were recovered by isoelectric precipitation, obtaining the F-V fraction (Supplementary Fig. 1). As with the second precipitation step, the third extraction showed optimal biomass recovery at approximately pH 3.8, with yields decreasing as the pH deviated from the protein's isoelectric point. In this stage, the highest yield was observed at a solubilisation pH of 2.0 (0.6 g·100 g^{-1}) compared to 0.4 g·100 g^{-1} obtained at pH 2.25 and 2.5. The protein content was also highest at pH 2.0 (0.03 g·100 g^{-1}), accompanied by an ash content of 0.45 g·100 g^{-1}. Overall, in terms of protein recovery from the leftovers of the phycobiliprotein recovery, the synergistic effect of an alkaline solubilisation pH of 12.0, and acidic solubilisation at a pH of 2.0 followed by precipitation at pH 3.8, proved to be the optimal balance, yielding the greatest overall recovery. These results indicate that maximal recovery at each extraction stage occurs when solubilisation is performed at pH values most distal from the isoelectric point. At these extremes (pH 2.0 or 12.0), proteins reach their maximum net electrical charge, promoting intense electrostatic repulsion and protein-solvent interaction, which maximises solubility. In contrast, the precipitation stages were designed to minimise the net charge, thereby overcoming the electrostatic repulsion and favouring aggregation. At the isoelectric point, hydrophobic interactions and van der Waals forces dominate, promoting efficient precipitation. Collectively, these findings highlight the critical role of precise pH control in optimising protein isolation.

Based on the results obtained in the "Ultrasound-assisted recovery of phycobiliproteins" and "Protein recovery from phycobiliprotein-extraction leftovers" sections, a biorefinery protocol was established. This consisted of ultrasound-assisted phycobiliprotein extraction at an initial biomass concentration of 100 g·L^{-1} and pH 8.0. Subsequently, isoelectric precipitation of the solubilised fraction at pH 4.3 was applied to obtain the B-PE-rich fraction (F-I). The remaining residue underwent alkaline protein solubilisation at pH 12.0, followed by a second isoelectric precipitation at pH 3.8 to recover the protein-rich fraction (F-II). In addition, an acidic solubilisation step at pH 2.0, followed by precipitation at pH 3.8 to obtain the F-V fraction (Supplementary Fig. 1), was evaluated as being the optimal downstream step. The importance of this third extraction stage, and the effect of liquid-phase reuse over the different recovery steps, are discussed in the following section.

Effect of Supernatant Reuse on the Protein Recovery Yield

To optimise the process, liquid-phase reuse was evaluated over the second and third extraction steps to assess its effect on the recovery of the F-II and F-V fractions (Supplementary Fig. 1; red line). Reintroducing the liquid fractions obtained after phycobiliprotein and protein precipitation back into the process substantially reduced water consumption while maintaining overall biomass recovery. The results indicate that the reutilisation of L-I, obtained after B-PE precipitation, led to a protein recovery in the second extraction step (F-II) of 10.8 g·100 g^{-1}. This value was 28.6% higher than that achieved when using fresh distilled water (8.4 g·100 g^{-1}; $p < 0.05$). The third fraction (F-V, Supplementary Fig. 1) was recovered in similar proportions when using distilled water and L-II, demonstrating that L-II reuse did not further improve protein recovery. However, recirculation did reduce the water input by 61%, while slightly enhancing

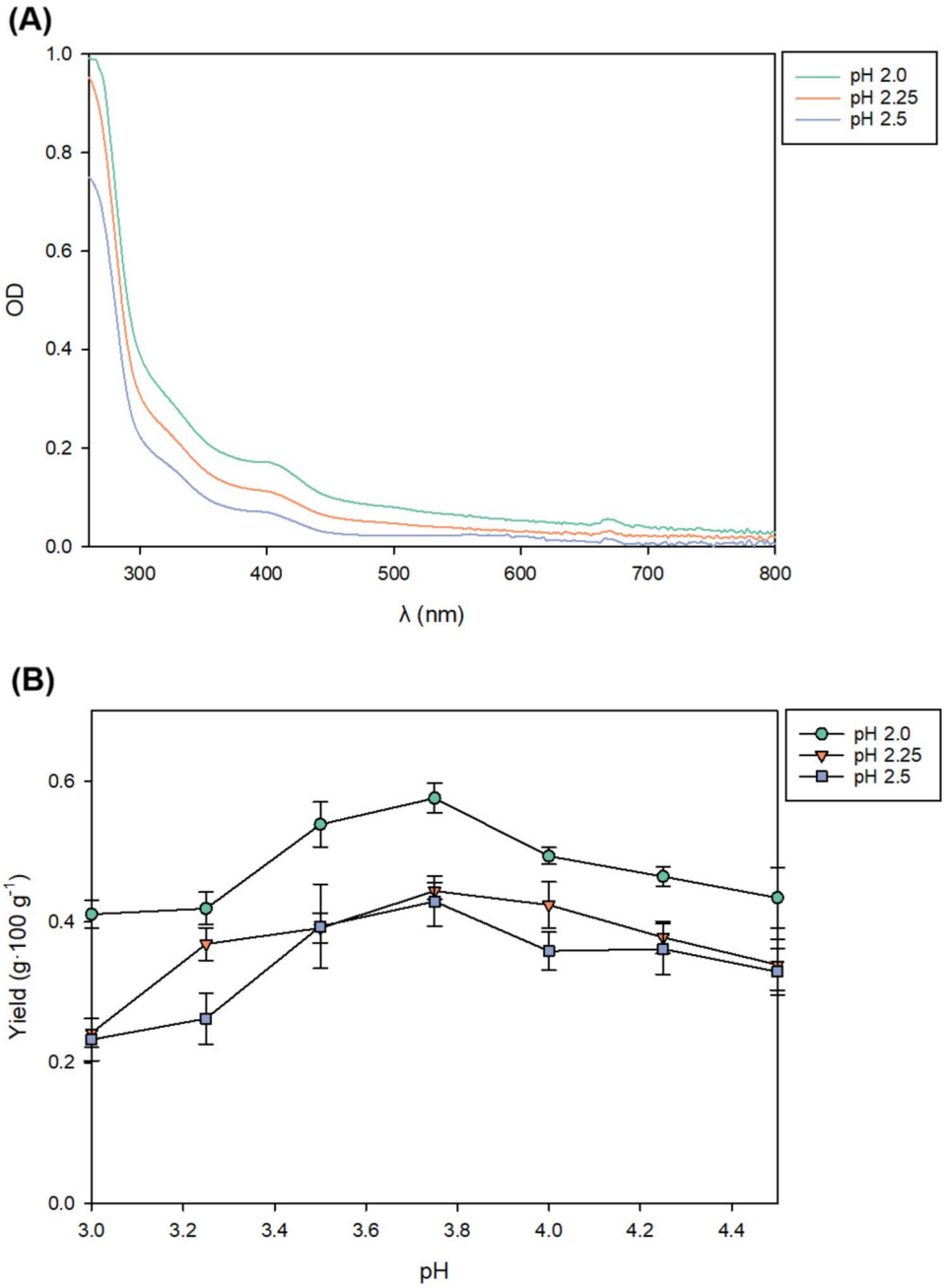


Fig. 4 Third extraction. **A** Effect of acidic pH on protein solubilisation; **B** absorbance spectra of the extracts under extremely acidic conditions; and **C** effect of precipitation pH on yield during the acidic step. Values correspond to the mean of three independent measurements ± SD

total extraction yield. These findings demonstrate that liquid-phase reuse is a viable strategy for improving resource efficiency and advancing the performance of microalgal biorefineries without compromising the recovery.

The protein content of the fractions after recirculation was 49.5, 56.0, and 10.1 g·100 g^{-1} for F-I, F-II and F-V, respectively. F-I and F-II had protein contents comparable to those of other protein-rich ingredients, including Sioux soy flour, 49.0 g·100 g^{-1} (Verfaillie et al., 2023); white bean extract, 45.1 g·100 g^{-1}; and chickpea extract, 49.9 g·100 g^{-1} (Calcinai et al., 2022). F-V (Supplementary Fig. 1) had a high mineral content (40.1 g·100 g^{-1}). Its inorganic composition included all the main dietary elements (Na, Mg, P, S, K, Ca, Cr, Mn, Fe, Cu, and Zn) involved in metabolic, enzymatic, and antioxidant functions (Gharibzahedi & Jafari, 2017). The resulting profile revealed a diversified mineral spectrum. Compared with previously reported mineral profiles of chlorella-based residues (Chang et al., 2015), the F-V fraction showed lower absolute concentrations in general but a broader and more diversified mineral composition. In the fraction obtained, Ca, P, Na, and Fe were the most abundant elements at 357.5, 107.1, 82.2, and 37.4 mg·kg^{-1}, respectively, while Mg, S, Mn, Zn, Cr, and Cu appeared at moderate to low levels but remained within nutritionally relevant

ranges. This difference might be attributed to the culture medium characteristics and the processing methods. The balanced inorganic profile indicated that F-V could be suitable for feedstock used in char production, offering potential environmental benefits by enhancing carbon sequestration and improving soil fertility, and for potential use as a complementary ingredient in functional formulations (Chaiwong et al., 2013; Prates, 2025). Nevertheless, to clarify its suitability for food and feed applications, further work needs to be carried out to assess bioaccessibility and regulatory feasibility.

Although liquid-phase reuse improved protein recovery and reduced water consumption throughout the process, the contribution made by the third extraction step to overall recovery remained limited, even under recirculation conditions. Consequently, terminating the process after the recovery of the F-II fraction was considered the most efficient and practical approach. A summary of the optimised process is shown in Fig. 1.

Functional Properties of the Recovered Fractions

Colouring Capacity of F-I

The F-I colouring performance was assessed in several food and beverage matrices covering a pH range of 2.4–6.1. The goal was to imitate the colour of commercial products pigmented using synthetic or plant-derived extracts. For the gin samples (Fig. 5A and B), the product containing concentrations of 1.4 and 0.9 mg B-PE·L^{-1} yielded ΔE* values of 5.2 and 3.6, respectively. Cserhalmi et al. (2006) classified colour differences as a function of ΔE* values into five levels: imperceptible (0–0.5), barely perceptible (0.05–1.5), perceptible (1.5–3.0), clearly perceptible (3.0–6.0), and highly noticeable (6.0–12.0).

This means that the gins coloured using the commercial and the microalgae-derived pigments showed a clearly perceptible colour difference. This does not signify that the colour had a higher or lower acceptance since this would need to be assessed in future works. Tonic waters (Fig. 5C and D) showed minimum ΔE* values of 5.3 and 9.5 between the F-I-coloured and the Fentimans Rose or Schweppes Pink tonic waters. These values were achieved when adding 0.1 and 1.8 mg B-PE·L^{-1}, respectively. The notable difference could be attributed to the presence of mixed pigments (anthocyanins, carrot and safflower extracts) in the commercial product. A similar characteristic was observed for gelatines (Fig. 5E and F), where the minimal colour differences were 6.2 and 13.6 between the F-I-coloured and the AllPure or Royal gelatines, when adding 1.8 and 2.6 mg B-PE·kg^{-1} product, respectively. The colour differences were clearly perceptible to the human eye. These results are comparable to previous studies reported for B-PE extract used to mimic the colour of pink gins, where the colour difference was approximately 2.6 after the incorporation of less than 2.0 mg B-PE·L^{-1} product (Carmona et al., 2022). The incorporation of algae-derived phycocyanin resulted in ΔE* values ranging from 5.0 to 10.0 compared with commercial blue isotonic drinks (García et al., 2021). Despite these results, the stability of B-PE within food matrices must be evaluated further — this is because pH can influence the protonation of chromophore-associated residues, potentially altering both colour and structural integrity. Although some studies suggest that B-PE extract maintains its native structure and its pink colour between pH 4.0 and 10.0, with a 10–15% colour loss at neutral pH after 2 weeks at room temperature and light exposure, more acidic conditions (pH < 4.0) induce partial unfolding, causing a slight shift in hue towards purple. Below pH 2.5, however, fluorescence is largely lost (González-Ramírez et al., 2014). Moreover, since a purity step was not carried out, the presence of salts and other compounds might interact with the protein or its chromophores, potentially altering the pigment's conformation, which may reduce the colour stability or modify absorbance in food matrices. Previous studies have shown that metal ions such as Fe^{3+}, Cu^{2+}, and Mn^{2+} can significantly attenuate the colour of phycoerythrin (Sun et al., 2023). Therefore, the combined effects of pH shifts and residual matrix components underscore the need to carefully evaluate B-PE stability in food systems.

The strong pigmentation capacity of F-I highlighted its potential as an alternative to synthetic dyes, in line with the rising demand for naturally derived pigments and clean label products. Microalgae-based colourants also offer key advantages over plant sources; these include rapid growth, minimal land requirements, and production in closed photobioreactors, which avoid limitations associated with soil availability and quality, climate, and seasonality (Novoveská et al., 2023). However, it is not yet authorised as a food additive. In the European Union, approval requires assessment under the Novel Foods Regulation (EU) 2015/2283. Nevertheless, recent studies do support the feasibility of using *P. cruentum* in both animal feed and human food products. For example, B-PE has been incorporated into a skimmed-milk beverage, improving the formulation's antioxidant capacity, providing higher sensory acceptance, and being demonstrated as non-toxic (Galetovic et al., 2020). Another study looking at C-phycoerythrin demonstrated its protective effects against oxidative DNA damage in rats (Soni et al., 2010).

Additionally, regulatory precedents in the EU food applications, such as the approval of astaxanthin from *Haematococcus pluvialis* as a food supplement, illustrate a potential pathway for the future authorisation of *P. cruentum* biomass.

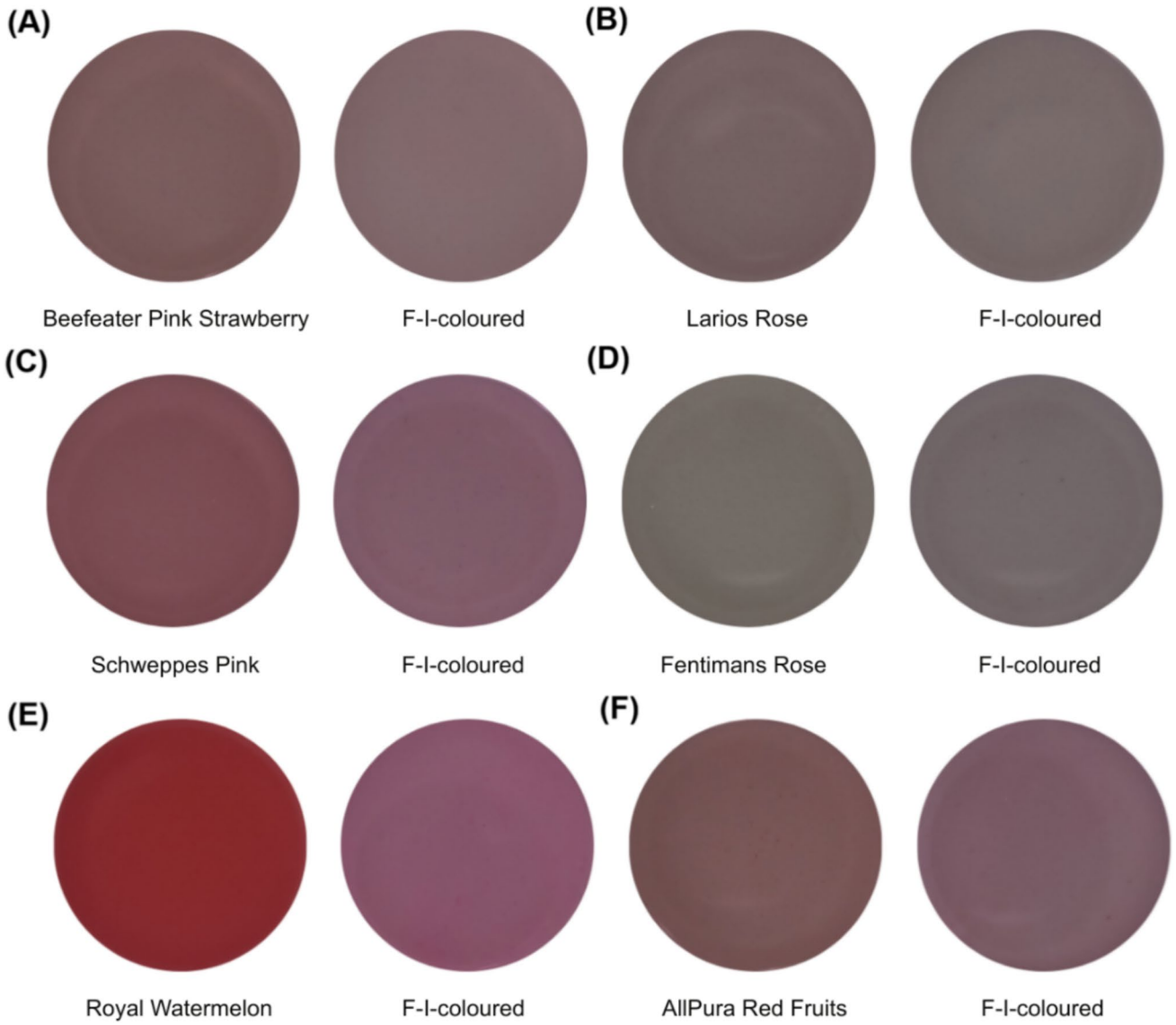


Fig. 5 Evaluation of the colouring performance of the B-PE–rich extract F-I compared to commercial products: gin (**A**) and (**B**), tonic water (**C**) and (**D**), and gelatine (**E**) and (**F**)

Emulsifying Capacity of F-II

Emulsions consist of two immiscible liquid phases that have inherently limited stability. In oil–water systems, emulsions rely on surface-active molecules capable of stabilising the interface between the oil and water (Taragjini et al., 2022). The emulsifying capacity and the emulsion stability of F-II, obtained using the optimised diagram shown in Fig. 1, were compared with commercial potato protein concentrate (this was selected as a reference because it is a plant-derived alternative with an established presence in the food market). The emulsifying capacity of F-II was strongly influenced by pH ($p < 0.05$), reaching its maximum at pH 8.0 (70%; Fig. 6A).

Any deviations from neutrality markedly reduced its performance, and no emulsion was observed at low pH values (2.0 and 4.0). The potato protein isolate displayed a lower but more uniform emulsion capacity profile (around 60%) across all pH levels. Similar pH-driven behaviour has been observed for *Nannochloropsis gaditana*, where the maximum emulsifying capacity (70%) occurred at pH 6.0. In that same study, the capacity ranged from 55 to 65% at pH 5.0–11.0, whereas it decreased markedly to 12% at pH 4.0 (Pino et al., 2025). In a study carried out by Benelhadj et al. (2016), a maximal emulsifying capacity of approximately 65% was obtained at pH 10.0 when using proteins isolated from *A. platensis*. Variations in the emulsifying capacity may be the result of differences in the extraction techniques

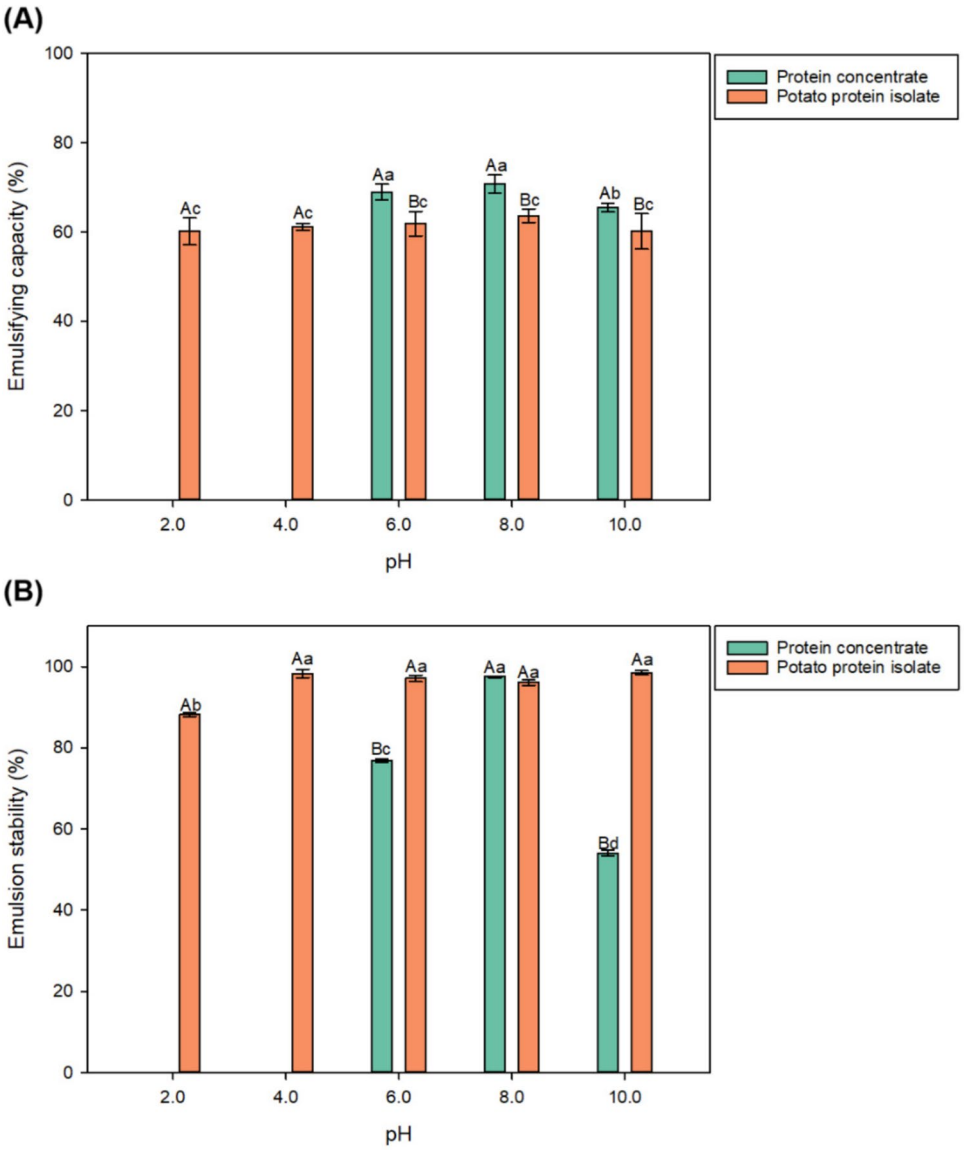


Fig. 6 (**A**) Emulsifying capacity of F-II and (**B**) emulsion stability. Uppercase letters show differences between proteins at a given pH. Lowercase letters show differences across pH values for the same protein. Values correspond to the mean of three independent measurements ± SD

and conditions, the strains employed, or the composition of the culture media, since these factors can significantly influence the proteins' techno-functional properties (Ursu et al., 2014). The high emulsifying capacity observed around neutral and alkaline pH, and the decrease seen towards extreme pH values, is consistent with the solubility of proteins at different pH values. This behaviour can influence the emulsifying capacity via mechanisms such as film formation or the interplay between Van der Waals attractions and electrostatic repulsions (Guil-Guerrero et al., 2004). Specifically, the emulsifying capacity of F-II remained statistically comparable between pH 6.0 and 8.0, whereas a significant decrease was observed at pH 10. This suggests that near-neutral conditions favour a balanced charge-to-hydrophobicity ratio, allowing for efficient protein adsorption and the formation of a cohesive interfacial film. Although solubility increases at higher pH, the reduced emulsifying capacity at pH 10.0 likely results from excessive electrostatic repulsion and extreme protein unfolding. These factors can prevent dense molecular packing at the oil–water interface, leading to a thinner and less robust film that is unable to stabilise a larger interfacial area (Wilde, 2000).

The thermal stability of the emulsions made with F-II exhibited a strong pH-dependence (Fig. 6B). Maximum stability was observed at pH 8.0 (98%), whereas both acidic (pH 6.0, 77%) and alkaline conditions (pH 10.0, 54%) significantly reduced emulsion stability against thermal stress ($p < 0.05$). Although the protein fraction became more soluble at high pH values, excessive charge and structural unfolding at extreme pH values likely disrupted molecular packing at the oil–water interface and led to a less cohesive and viscoelastic interfacial film. Because emulsion stability

depends on the interfacial structure, droplet interactions, and density differences between the oil and aqueous phases, changes in these properties can diminish the system's resistance to thermal stress (Han et al., 2020). Overall, the results indicate that *P. cruentum* protein concentrate (F-II) shows potential as a food-grade emulsifier, particularly under near-neutral to moderately alkaline conditions. Even though the fractions obtained are not crude extracts, isoelectric precipitation fails to yield a purified protein isolate. Consequently, the resulting fractions may still contain non-protein compounds such as salts, pigments, lipids, or polysaccharides. Studies on microalgae have shown that such co-extracted compounds can influence the functional properties of the protein fractions, particularly in the presence of surfactants. For example, Buchmann et al. (2019) as reported that crude extracts of *A. platensis* exhibited reduced foam expansion and increased bubble dimensions relative to whey protein isolate. In contrast, the purified protein isolate achieves superior overrun while maintaining a bubble size comparable to the whey protein isolate. Performance can be significantly improved by defatting, which removes oil-soluble surfactants that would otherwise compete with proteins for interfacial adsorption (Bertsch et al., 2021).

Biostimulant Capacity of F-III

The utilisation of F-III and L-II, obtained following the optimised protocol shown in Fig. 1, led to an increase in the cucumber seedling vigour index ($p < 0.05$) whereas no significant difference was observed for basil seeds (Fig. 7).

The graph illustrates the percentage increase relative to distilled water alone. The F-III fraction led to the greatest improvement in the seedling vigour index (55%), followed by L-II (51%). Across all the treatments using *Porphyridium cruentum* extracts, the index increased by 36–55%, indicating a substantial improvement compared to water alone. Furthermore, all the solubilised microalgae-derived fractions outperformed the positive control (although it was used at a lower concentration). Comparable findings were reported for the microalga *Oscillatoria* sp., with the residual biomass obtained after C-phycocyanin extraction showing potential as a biostimulant of watercress seeds (Morillas-España et al., 2022). In the present study, all the basil treatments showed improvements in the vigour index with increases ranging from 11 to 26%, similar to those for the positive control. The dissimilar responses observed between the seed species could be attributed to differences in the specific physiological requirements for germination. The response to exogenous hormones, such as gibberellic acid, or the microalgae compounds is highly species- and dose-dependent. For instance, gibberellic acid at a concentration of 100 mg·L^{-1} has been shown to enhance sweet basil germination by 32.6% compared to the control (Elhindi et al., 2016). In the present study, low concentrations of gibberellic acid and potential growth-promoting compounds were tested; therefore, the evaluation of additional concentrations may be necessary

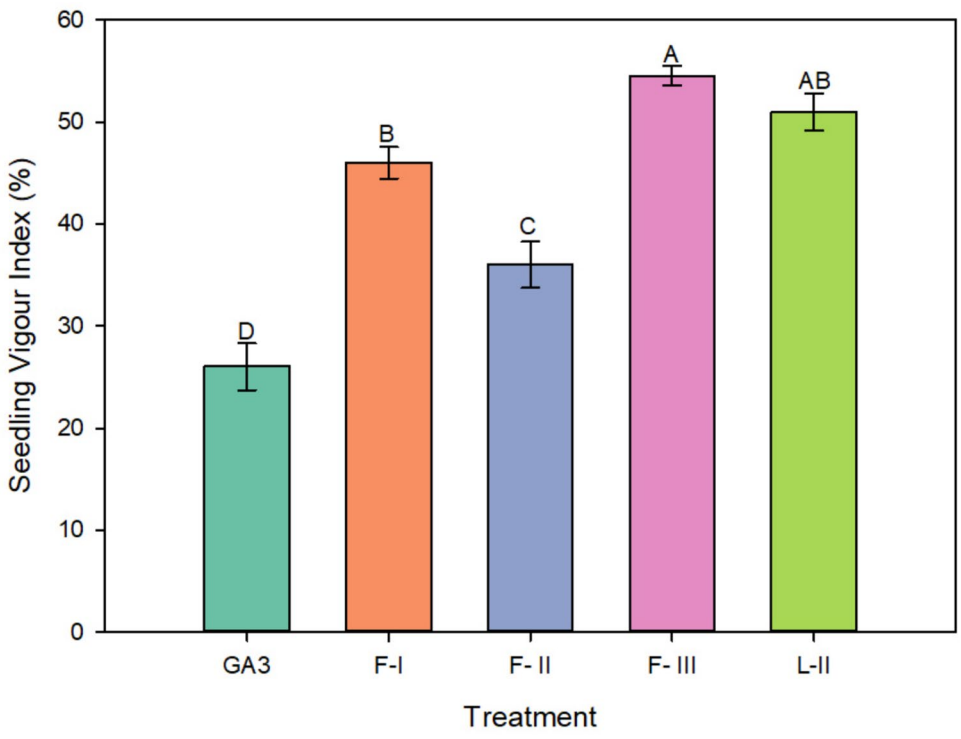


Fig. 7 Seedling vigour index of cucumber treated with the obtained fractions. Values are expressed as a percentage relative to the distilled-water control. Values correspond to the mean of three independent measurements ± SD. GA3 corresponds to gibberellic acid (the positive control) assessed at a concentration of 1 mg·L^{-1}. FI-FIII and L-II correspond to the different fractions obtained following the optimised scheme shown in Fig. 1. These fractions were assessed at a concentration of 0.5 g·L^{-1}

to determine early potential growth improvement in some species.

Such species-specific behaviour indicates that biostimulant activity is dependent on plant type and metabolic sensitivity to the applied compounds, concentrations, and strains.

Overall, the findings described here suggested that all fractions, and particularly the leftovers from protein extraction, show potential as plant biostimulants. Nevertheless, future studies are required to elucidate the mechanisms responsible for these early growth-promoting effects and to identify the dose that yields the greatest response.

Conclusions

This work sets out a novel strategy for the comprehensive valorisation of *P. cruentum* biomass. Ultrasound-assisted extraction at high biomass concentrations, followed by controlled alkaline and acidic solubilisation/precipitation, maximised pigment and protein release. The reuse of the liquid stream back into the extraction process reduced water consumption without compromising protein recovery. The resulting fractions exhibited relevant functional properties, supporting their application as natural colourants, emulsifiers, and plant biostimulants. Although an additional acidic extraction step was evaluated, its contribution to the total protein recovery was limited, making the two-step extraction a more efficient and practical approach. These results demonstrate the significant potential of circular and resource-efficient microalgal biorefineries; nevertheless, further research is required to refine the extraction times and improve the purity of the extracts. Overall, the results highlight the potential of *P. cruentum* as a versatile source of high-, medium-, and low-value products, which align with circular economy principles and support the development of sustainable microalgae-based ingredients.

Supplementary Information The online version contains supplementary material available at https://doi.org/10.1007/s11947-026-04322-0.

Author Contribution Cáceres-Ferroni, F.: Writing – original draft, Investigation, Formal Analysis; Salinas-García, M.: Investigation; Villaró-Cos, S.: Investigation; Rivera, E.: Investigation; Lafarga, T.: Writing – review & editing, Investigation, Supervision, Funding acquisition.

Funding Funding for open access publishing: Universidad de Almería/CBUA. This work is part of the SOLAR·FOODS (PID2022-136292OB-I00) and SHAPE (CNS2024-154218) projects, funded by the Spanish Ministry of Science and Innovation MCIN/AEI/https://doi.org/10.13039/501100011033and the European Union's NextGenerationEU/PRTR. This work also forms part of the BLUE·FUTURE (PCM_00083) project, funded by the Government of Andalusia and the European Union's NextGenerationEU/PRTR. The manuscript is also supported by the Circular Bio-based Europe Joint Undertaking and its member, and co-funded by the EU (Grant No. 101214199).

Data Availability Data will be made available on reasonable request from the corresponding author.

Declarations

Conflict of interest The authors declare no competing interests.

Open Access This article is licensed under a Creative Commons Attribution 4.0 International License, which permits use, sharing, adaptation, distribution and reproduction in any medium or format, as long as you give appropriate credit to the original author(s) and the source, provide a link to the Creative Commons licence, and indicate if changes were made. The images or other third party material in this article are included in the article's Creative Commons licence, unless indicated otherwise in a credit line to the material. If material is not included in the article's Creative Commons licence and your intended use is not permitted by statutory regulation or exceeds the permitted use, you will need to obtain permission directly from the copyright holder. To view a copy of this licence, visit http://creativecommons.org/licenses/by/4.0/.

References

AENOR. (2022). *DIN EN 17605:2022-07: Algae and algae products - Methods of sampling and analysis - Sampling treatment.*

Alting, A. C., Pouvreau, L., Giuseppin, M. L. F., & van Nieuwenhuijzen, N. H. (2011). Potato proteins. In *Handbook of food proteins*, 316–334. https://doi.org/10.1533/9780857093639.316

Ardila-Leal, L. D., Poutou-Piñales, R. A., Pedroza-Rodríguez, A. M., & Quevedo-Hidalgo, B. E. (2021). A brief history of colour, the environmental impact of synthetic dyes and removal by using laccases. *Molecules, 26*(13), Article 3813. https://doi.org/10.3390/molecules26133813

Benelhadj, S., Gharsallaoui, A., Degraeve, P., Attia, H., & Ghorbel, D. (2016). Effect of pH on the functional properties of Arthrospira (Spirulina) platensis protein isolate. *Food Chemistry, 194*, 1056–1063. https://doi.org/10.1016/j.foodchem.2015.08.133

Bermejo, R., Talavera, E. M., & Alvarez-Pez, J. M. (2001). Chromatographic purification and characterization of B-phycoerythrin from *Porphyridium cruentum*. *Journal of Chromatography A, 917*(1–2), 135–145. https://doi.org/10.1016/S0021-9673(01)00660-9

Bermejo-Román, R., Murillo-Cruz, M. C., Hurtado, M. C., Villaró-Cos, S., Lafarga, T., & Acién, G. (2025). Simplified two-stage method for the recovery of B-phycoerythrin from Porphyridium cruentum and evaluation as a natural food grade colourant. *Food and Bioprocess Technology, 18*, 6743–6751. https://doi.org/10.1007/s11947-025-03859-w

Bernaerts, T. M. M., Kyomugasho, C., Van Looveren, N., Gheysen, L., Foubert, I., Hendrickx, M. E., & Van Loey, A. M. (2018). Molecular and rheological characterization of different cell wall fractions of *Porphyridium cruentum*. *Carbohydrate Polymers, 195*, 542–550. https://doi.org/10.1016/j.carbpol.2018.05.001

Bertsch, P., Böcker, L., Mathys, A., & Fischer, P. (2021). Proteins from microalgae for the stabilization of fluid interfaces, emulsions, and foams. *Trends in Food Science & Technology, 108*, 326–342. https://doi.org/10.1016/j.tifs.2020.12.014

Biró-Janka, B., Nyárádi, I.-I., Duda, M. M., Demeter, B., & Nagy-György, A. (2019). Changes in germination parameters of seven sweet basil (*Ocimum basilicum* L.) varieties due to treating with gibberellic and ascorbic acids. *Acta Universitatis Sapientiae, Agriculture and Environment, 11*, 83–94. https://doi.org/10.2478/ausae-2019-0008

Boada, L. D., Henríquez-Hernández, L. A., & Luzardo, O. P. (2016). The impact of red and processed meat consumption on cancer and other health outcomes: Epidemiological evidences. *Food and Chemical Toxicology, 92*, 236–244. https://doi.org/10.1016/j.fct.2016.04.008

Buchmann, L., Bertsch, P., Böcker, L., Krähenmann, U., Fischer, P., & Mathys, A. (2019). Adsorption kinetics and foaming properties of soluble microalgae fractions at the air–water interface. *Food Hydrocolloids, 97*, Article 105182. https://doi.org/10.1016/j.foodhyd.2019.105182

Cáceres-Ferroni, F., Salinas-García, M., Villaró-Cos, S., Rivera-Sánchez, E., & Lafarga, T. (2025). Effect of culture medium composition and reuse on the growth of Porphyridium cruentum. *New Biotechnology, 90*, 65–76. https://doi.org/10.1016/j.nbt.2025.09.001

Calcinai, L., Bonomini, M. G., Leni, G., Faccini, A., Puxeddu, I., Giannini, D., Petrelli, F., Prandi, B., Sforza, S., & Tedeschi, T. (2022). Effectiveness of enzymatic hydrolysis for reducing the allergenic potential of legume by-products. *Scientific Reports, 12*, Article 16902. https://doi.org/10.1038/s41598-022-21296-z

Camara-Artigas, A., Bacarizo, J., Andujar-Sanchez, M., Ortiz-Salmeron, E., Mesa-Valle, C., Cuadri, C., Martin-Garcia, J. M., Martinez-Rodriguez, S., Mazzuca-Sobczuk, T., Ibáñez, M. J., & Allen, J. P. (2012). pH-dependent structural conformations of B-phycoerythrin from *Porphyridium cruentum*. *FEBS Journal, 279*(19), 3680–3691. https://doi.org/10.1111/j.1742-4658.2012.08730.x

Carmona, R., Murillo, M. C., Lafarga, T., & Bermejo, R. (2022). Assessment of the potential of microalgae-derived phycoerythrin as a natural colorant in beverages. *Journal of Applied Phycology, 34*, 3025–3034. https://doi.org/10.1007/s10811-022-02834-8

Chabili, A., Hakkoum, Z., Minaoui, F., Douma, M., Meddich, A., & Loudiki, M. (2025). Germination screen of eco-extracts from soil cyanobacteria and microalgae for their biostimulant effects on wheat seed emergence and vigor. *Algal Research, 89*, Article 104087. https://doi.org/10.1016/j.algal.2025.104087

Chaiwong, K., Kiatsiriroat, T., Vorayos, N., & Thararax, C. (2013). Study of bio-oil and bio-char production from algae by slow pyrolysis. *Biomass and Bioenergy, 56*, 600–606. https://doi.org/10.1016/j.biombioe.2013.05.035

Chang, Y. M., Tsai, W. T., & Li, M. H. (2015). Chemical characterization of char derived from slow pyrolysis of microalgal residue. *Journal of Analytical and Applied Pyrolysis, 111*, 88–93. https://doi.org/10.1016/j.jaap.2014.12.004

Chegukrishnamurthi, M., Nagarajan, S., Ravi, S., Mudliar, S. N., & Ranade, V. V. (2025). Hydrodynamic cavitation mediated Spirulina valorisation with insights into phycocyanin extraction and biogas production. *Communications Biology, 8*, Article 326. https://doi.org/10.1038/s42003-025-07702-y

Chen, Y., Chen, J., Chang, C., Chen, J., Cao, F., Zhao, J., Zheng, Y., & Zhu, J. (2019). Physicochemical and functional properties of proteins extracted from three microalgal species. *Food Hydrocolloids, 96*, 510–517. https://doi.org/10.1016/j.foodhyd.2019.05.025

Cserhalmi, Z., Sass-Kiss, Á., Tóth-Markus, M., & Lechner, N. (2006). Study of pulsed electric field treated citrus juices. *Innovative Food Science & Emerging Technologies, 7*(1–2), 49–54. https://doi.org/10.1016/j.ifset.2005.07.001

Dai, L., Reichert, C. L., Hinrichs, J., & Weiss, J. (2019). Acid hydrolysis behavior of insoluble protein-rich fraction extracted from Chlorella protothecoides. *Colloids and Surfaces A: Physicochemical and Engineering Aspects, 569*, 129–136. https://doi.org/10.1016/j.colsurfa.2019.02.064

Damodaran, S., & Paraf, A. (2017). *Food proteins and their applications* (1st ed.). CRC Press. https://doi.org/10.1201/9780203755617

Elhindi, K. M., Dewir, Y. H., Asrar, A.-W., Abdel-Salam, E., El-Din, A. S., & Ali, M. (2016). Improvement of seed germination in three medicinal plant species by plant growth regulators. *HortScience, 51*(7), 887–891. https://doi.org/10.21273/HORTSCI.51.7.887

Ferreira, A. S., Mendonça, I., Póvoa, I., Carvalho, H., Correia, A., Vilanova, M., Silva, T. H., Coimbra, M. A., & Nunes, C. (2021). Impact of growth medium salinity on galactoxylan exopolysaccharides of *Porphyridium purpureum*. *Algal Research, 59*, Article 102439. https://doi.org/10.1016/j.algal.2021.102439

Future Market Insights. (2024). Phycoerythrin market forecast to reach USD 10.3 million by 2034 [Internet document]. https://www.futuremarketinsights.com/. Accessed 01 Dec 2025.

Galetovic, A., Seura, F., Gallardo, V., Graves, R., Cortés, J., Valdivia, C., Nuñez, J., Tapia, C., Neira, I., Sanzana, S., & Gómez-Silva, B. (2020). Use of phycobiliproteins from Atacama cyanobacteria as food colorants in a dairy beverage prototype. *Foods, 9*(2), Article 244. https://doi.org/10.3390/foods9020244

García, A. B., Longo, E., & Bermejo, R. (2021). The application of a phycocyanin extract obtained from Arthrospira platensis as a blue natural colorant in beverages. *Journal of Applied Phycology, 33*, 3059–3070. https://doi.org/10.1007/s10811-021-02522-z

Garcia-Vaquero, M., Lopez-Alonso, M., & Hayes, M. (2017). Assessment of the functional properties of protein extracted from the brown seaweed Himanthalia elongata (Linnaeus) S. F. Gray. *Food Research International, 99*, 971–978. https://doi.org/10.1016/j.foodres.2016.06.023

George, R., & John, J. A. (2023). Phycoerythrin as a potential natural colourant: A mini review. *International Journal of Food Science & Technology, 58*(2), 513–519. https://doi.org/10.1111/ijfs.16229

Gharibzahedi, S. M. T., & Jafari, S. M. (2017). The importance of minerals in human nutrition: Bioavailability, food fortification, processing effects and nanoencapsulation. *Trends in Food Science & Technology, 62*, 119–132. https://doi.org/10.1016/j.tifs.2017.02.017

Ghedifa, A. B., Vega, J., Korbee, N., Mensi, F., Figueroa, F. L., & Sadok, S. (2021). Effects of light quality on the photosynthetic activity and biochemical composition of Gracilaria gracilis (Rhodophyta). *Journal of Applied Phycology, 33*, 3413–3425. https://doi.org/10.1007/s10811-021-02496-y

Glazer, A. N. (1989). Light guides: Directional energy transfer in a photosynthetic antenna. *Journal of Biological Chemistry, 264*, 1–4. PMID: 2491842.

González-Ramírez, E., Andújar-Sánchez, M., Ortiz-Salmerón, E., Bacarizo, J., Cuadri, C., Mazzuca-Sobczuk, T., Ibáñez, M. J., Cámara-Artigas, A., & Martínez-Rodríguez, S. (2014). Thermal and pH stability of the B-phycoerythrin from the red algae *Porphyridium cruentum*. *Food Biophysics, 9*, 184–192. https://doi.org/10.1007/s11483-014-9331-x

Grossmann, L., Ebert, S., Hinrichs, J., & Weiss, J. (2018). Effect of precipitation, lyophilization, and organic solvent extraction on preparation of protein-rich powders from the microalgae Chlorella protothecoides. *Algal Research, 29*, 266–276. https://doi.org/10.1016/j.algal.2017.11.019

Guil-Guerrero, J. L., Navarro-Juárez, R., López-Martínez, J. C., Campra-Madrid, P., & Rebolloso-Fuentes, M. (2004). Functional properties of the biomass of three microalgal species. *Journal of Food Engineering, 65*(4), 511–517. https://doi.org/10.1016/j.jfoodeng.2004.02.014

Hadinoto, K., Ling, J.-U., Pu, S., & Tran, T.-T. (2024). Effects of alkaline extraction pH on amino acid compositions, protein secondary structures, thermal stability, and functionalities of brewer's spent grain proteins. *International Journal of Molecular Sciences, 25*(12), Article 6369. https://doi.org/10.3390/ijms25126369

Hampton, J. G. & Tekrony, D. M. (1995). *Handbook of vigor test methods*. International Seed Testing Association (ISTA).

Han, J., Chen, F., Gao, C., Zhang, Y., & Tang, X. (2020). Environmental stability and curcumin release properties of Pickering emulsion

stabilized by chitosan/gum arabic nanoparticles. *International Journal of Biological Macromolecules, 157*, 202–211. https://doi.org/10.1016/j.ijbiomac.2020.04.177

Koller, K. P., & Wehrmeyer, W. (1975). B-Phycoerythrin from *Rhodella violacea*. *Archives of Microbiology, 104*, 255–261. https://doi.org/10.1007/BF00447334

Kulkarni, S., & Nikolov, Z. (2018). Process for selective extraction of pigments and functional proteins from *Chlorella vulgaris*. *Algal Research, 35*, 185–193. https://doi.org/10.1016/j.algal.2018.08.024

Liu, F., Chen, Z., Wang, L., & Wang, R. (2013). Effects of protein solubilisation and precipitation pH values on the functional properties of defatted wheat germ protein isolates. *International Journal of Food Science & Technology, 48*(7), 1490–1497. https://doi.org/10.1111/ijfs.12117

Liu, Y., Liu, X., Cui, Y., & Yuan, W. (2022). Ultrasound for microalgal cell disruption and product extraction: A review. *Ultrasonics Sonochemistry, 87*, Article 106054. https://doi.org/10.1016/j.ultsonch.2022.106054

Lowry, O. H., Rosebrough, N. J., Farr, A. L., & Randall, R. J. (1951). Protein measurement with the Folin phenol reagent. *Journal of Biological Chemistry, 193*, 265–275. PMID: 14907713.

Mittal, R., Sharma, R., & Raghavarao, K. (2019). Aqueous two-phase extraction of R-Phycoerythrin from marine macro-algae, *Gelidium pusillum*. *Bioresource Technology, 280*, 277–286. https://doi.org/10.1016/j.biortech.2019.02.044

Morillas-España, A., Bermejo, R., Abdala-Díaz, R., Ruiz, Á., Lafarga, T., Acién, G., & Fernández-Sevilla, J. M. (2022). Biorefinery approach applied to the production of food colourants and biostimulants from *Oscillatoria* sp. *Biology, 11*(9), Article 1278. https://doi.org/10.3390/biology11101278

Morillas-España, A., Pérez-Crespo, R., Villaró-Co, s, Rodríguez-Chikri, L., & Lafarga, T. (2024). Integrating microalgae-based wastewater treatment, biostimulant production, and hydroponic cultivation: A sustainable approach to water management and crop production. *Frontiers in Bioengineering and Biotechnology, 12*, Article 1364490. https://doi.org/10.3389/fbioe.2024.1364490

Munier, M., Jubeau, S., Wijaya, A., Morançais, M., Dumay, J., Marchal, L., Jaouen, P., & Fleurence, J. (2014). Physicochemical factors affecting the stability of two pigments: R-phycoerythrin of *Grateloupia turuturu* and B-phycoerythrin of *Porphyridium cruentum*. *Food Chemistry, 150*, 400–407. https://doi.org/10.1016/j.foodchem.2013.10.113

Nath, P. C., Tiwari, O. N., Devi, I., Bandyopadhyay, T. K., & Bhunia, B. (2021). Biochemical and morphological fingerprints of isolated *Anabaena* sp.: A precious feedstock for food additives. *Biomass Conversion and Biorefinery, 11*, 2723–2733. https://doi.org/10.1007/s13399-020-00651-y

Nissen, S. H., Schmidt, J. M., Gregersen, S., Hammershøj, M., Møller, A. H., Danielsen, M., Stødkilde, L., Nebel, C., & Dalsgaard, T. K. (2021). Increased solubility and functional properties of precipitated alfalfa protein concentrate subjected to pH shift processes. *Food Hydrocolloids, 119*, Article 106874. https://doi.org/10.1016/j.foodhyd.2021.106874

Novoveská, L., Nielsen, S. L., Eroldoğan, O. T., Haznedaroglu, B. Z., Rinkevich, B., Fazi, S., Robbens, J., Vasquez, M., & Einarsson, H. (2023). Overview and challenges of large-scale cultivation of photosynthetic microalgae and cyanobacteria. *Marine Drugs, 21*(8), Article 445. https://doi.org/10.3390/md21080445

OECD. (2006). *Test No. 208: Terrestrial plant test: Seedling emergence and seedling growth test*. OECD Guidelines for Testing of Chemicals, Section 2. OECD Publishing. https://doi.org/10.1787/9789264070066-en

Patel, P., Pang, Y. L. J., Choi, W. J., & Wong, A. (2025). Protein extraction and isolation from legumes and algae: An industry primer. *Food and Bioprocess Technology, 18*, 8380–8408. https://doi.org/10.1007/s11947-025-03958-8

Piera, A., Espada, J. J., Morales, V., Rodríguez, R., Vicente, G., & Bautista, L. F. (2024). Optimised phycoerythrin extraction method from *Porphyridium* sp. combining imidazolium-based ionic liquids. *Heliyon, 10*(14), Article e34957. https://doi.org/10.1016/j.heliyon.2024.e34957

Pino, D., Castro-Varela, P., Morales, E., & Rubilar, M. (2025). Stability and emulsifying properties of water-soluble proteins from *Nannochloropsis gaditana* (Chlorophyta): Effects of pH, ionic strength, and temperature on single and double emulsions. *Algal Research, 92*, Article 104414. https://doi.org/10.1016/j.algal.2025.104414

Prates, J. A. M. (2025). The role of microalgae in providing essential minerals for sustainable swine nutrition. *Frontiers in Animal Science, 6*, 127–141. https://doi.org/10.3389/fanim.2025.1526433

Radnitz, C., Beezhold, B., & DiMatteo, J. (2015). Investigation of lifestyle choices of individuals following a vegan diet for health and ethical reasons. *Appetite, 90*, 31–36. https://doi.org/10.1016/j.appet.2015.02.026

Ryckebosch, E., Muylaert, K., & Foubert, I. (2012). Optimization of an analytical procedure for extraction of lipids from microalgae. *Journal of the American Oil Chemists' Society, 89*, 189–198. https://doi.org/10.1007/s11746-011-1903-z

Schmidt, J. M., Damgaard, H., Greve-Poulsen, M., Larsen, L. B., & Hammershøj, M. (2018). Foam and emulsion properties of potato protein isolate and purified fractions. *Food Hydrocolloids, 74*, 367–378. https://doi.org/10.1016/j.foodhyd.2017.07.032

Soni, B., Visavadiya, N. P., Dalwadi, N., Madamwar, D., Winder, C., & Khalil, C. (2010). Purified c-phycoerythrin: Safety studies in rats and protective role against permanganate-mediated fibroblast-DNA damage. *Journal of Applied Toxicology, 30*, 542–550. https://doi.org/10.1002/jat.1524

Stack, J., Le Gouic, A. V., Tobin, P. R., Guihéneuf, F., Stengel, D. B., & FitzGerald, R. J. (2018). Protein extraction and bioactive hydrolysate generation from two microalgae, Porphyridium purpureum and Phaeodactylum tricornutum. *Journal of Food Bioactives, 3*, 153–165. https://doi.org/10.31665/JFB.2018.1134

Sun, Y., Cui, Y., Wang, R., Ma, J., Sun, H., Cheng, L., & Yang, R. (2023). The hydrolysis of pigment–protein phycoerythrin by bromelain enhances the color stability. *Foods, 12*(13), Article 2574. https://doi.org/10.3390/foods12132574

Taragjini, E., Ciardi, M., Musari, E., Villaró, S., Morillas-España, A., Alarcón, F. J., & Lafarga, T. (2022). Pilot-scale production of A. platensis: Protein isolation following an ultrasound-assisted strategy and assessment of techno-functional properties. *Food and Bioprocess Technology, 15*, 1299–1310. https://doi.org/10.1007/s11947-022-02789-1

Tounsi, L., Ben Hlima, H., Elhadef, K., Hentati, O., Blavignac, C., Fendri, I., Smaoui, S., Michaud, P., & Abdelkafi, S. (2024). B-phycoerythrin of *Porphyridium cruentum* UTEX 161: A multifunctional active molecule for the development of biodegradable films. *European Polymer Journal, 208*, Article 112851. https://doi.org/10.1016/j.eurpolymj.2024.112851

Tsvetanova, F., & Yankov, D. (2022). Bioactive compounds from red microalgae with therapeutic and nutritional value. *Microorganisms, 10*(11), Article 2290. https://doi.org/10.3390/microorganisms10112290

United Nations. (2024). World population prospects 2024 [Internet document]. https://population.un.org/wpp/graphs?loc=900&type=Demographic%20Profiles&category=Line%20Charts. Accessed 01 Dec 2025.

Ursu, A.-V., Marcati, A., Sayd, T., Sante-Lhoutellier, V., Djelveh, G., & Michaud, P. (2014). Extraction, fractionation and functional properties of proteins from the microalgae *Chlorella vulgaris*. *Bioresource Technology, 157*, 134–139. https://doi.org/10.1016/j.biortech.2014.01.071

Verfaillie, D., Janssen, F., Van Royen, G., & Wouters, A. G. B. (2023). A systematic study of the impact of the isoelectric precipitation process on the physical properties and protein composition of soy protein isolates. *Food Research International, 163*, Article 112177. https://doi.org/10.1016/j.foodres.2022.112177

Villaró, S., Acién, G., González-López, C. V., Clagnan, E., & Lafarga, T. (2023). Production of *Arthrospira platensis* BEA 005B: Biomass characterisation and use as a colouring additive in macarons. *LWT, 182*, Article 114843. https://doi.org/10.1016/j.lwt.2023.114843

Villaró, S., Valero-Cardoso, S., Cerdá-Moreno, C., Ciardi, M., & Lafarga, T. (2025). Strategies to control the growth of unwanted microalgae during the production of *Arthrospira platensis* BEA 005B. *Cleaner Engineering and Technology, 27*, Article 101035. https://doi.org/10.1016/j.clet.2025.101035

Wilde, P. J. (2000). Interfaces: Their role in foam and emulsion behaviour. *Current Opinion in Colloid & Interface Science, 5*(3–4), 176–181. https://doi.org/10.1016/S1359-0294(00)00056-X

Xie, Y., Khoo, K. S., Chew, K. W., Devadas, V. V., Phang, S. J., Lim, H. R., Rajendran, S., & Show, P. L. (2022). Advancement of renewable energy technologies via artificial and microalgae photosynthesis. *Bioresource Technology, 363*, Article 127830. https://doi.org/10.1016/j.biortech.2022.127830

Publisher's Note Springer Nature remains neutral with regard to jurisdictional claims in published maps and institutional affiliations.